Synthesis and Reactivity of the Iridium(I) Mesityl Complex Ir(CO)(mes)(dppe). Oxidative Addition and Ligand Activation Reactions

Brian P. Cleary and Richard Eisenberg*

Contribution from the Department of Chemistry, University of Rochester, Rochester, New York 14627

Received October 13, 1994[⊗]

Abstract: The complex Ir(CO)(mes)dppe (**1**) (mes = 1,3,5-trimethylphenyl, dppe = 1,2-bis(diphenylphosphino)-ethane) has been synthesized from the reaction of IrBr(CO)(dppe) and mesitylmagnesium bromide. Complex **1** crystallizes in the monoclinic space group, $P2_1/n$ (No. 14), with $Z = 4$, $a = 8.953(3)$ Å, $b = 22.752(6)$ Å, $c = 16.212(6)$ Å, and $\beta = 99.00(3)°$, and displays a slight tetrahedral distortion from square planarity. A benzene solution of **1** undergoes an unusual transformation when heated to 90 °C under ethylene to form the five-coordinate dimethylbenzyl complex Ir(η^2-C_2H_4)($CH_2C_6H_3(CH_3)_2$)(CO)(dppe) (**2**) via *o*-methyl C−H activation. An X-ray determination of **2** shows that it crystallizes in the orthorhombic space group, *Pbca* (No. 61), with $Z = 8$, $a = 19.113(8)$ Å, $b = 16.243(9)$ Å, $c = 23.174(7)$ Å. Complex **1** under CO undergoes aryl migration to form the dicarbonyl adduct $Ir(CO)_2(C(O)C_6H_2(CH_3)_3)$(dppe) (**6**). After a benzene solution of complex **6** is heated, an equilibrium of *trans*-IrH(CO)($CH_2C_6H_2(CH_3)_2C(O)$)(dppe) (**7**), *cis*-IrH(CO)($CH_2C_6H_2(CH_3)_2C(O)$)(dppe) (**8**), and **6** is formed. Complexes **7** and **8** are formed by *o*-methyl C−H activation. A crystal structure determination of **8** shows that it crystallizes in the monoclinic space group $P2_1/n$ (No. 14), with $Z = 4$, $a = 10.701(3)$ Å, $b = 14.554(3)$ Å, $c = 20.760(6)$ Å, and $\beta = 90.19(3)°$. Solutions of complex **1** undergo stereospecific oxidative additions of HY (Y = $SiHPh_2$, H) to form IrH(Y)(CO)(mes)(dppe) (**9**) (Y = $SiHPh_2$) and **10** (Y = H), respectively. The complex IrI_2-$(C(O)C_6H_2(CH_3)_3)$(dppe), **11**, is formed when a benzene solution of **1** is treated with a benzene solution of I_2. Under HCl gas, a CD_2Cl_2 solution of **1** is readily converted to $IrHCl_2$(CO)(dppe) (**12**) and free mesitylene.

Introduction

The reaction of small molecules with four-coordinate d^8 metal centers plays a major role in homogeneous catalytic processes such as hydrogenation, hydrosilation, and hydroformylation.[1,2] In these processes, substrate activation occurs via coordination or oxidative addition and substrate transformation takes place through insertion, coupling, and reductive elimination steps. Examples of successful homogeneous catalysts include Wilkinson's catalyst, $RhCl(PPh_3)_3$, cationic rhodium complexes $[RhL_2S_2]^+$, where S = solvent, related asymmetric hydrogenation catalysts, where L_2 is a chiral chelating diphosphine, Crabtree's catalyst, $[Ir(COD)(P(Cy)_3)(Py)]PF_6$, and RhH(CO)-$(PPh_3)_3$.[3−20]

For the catalytic processes mentioned above, the rate of product formation is generally so fast that characterization of organometallic intermediates formed during the reaction is difficult. One approach to studying these reactions mechanistically is through the modeling of proposed intermediates with transition metal complexes that are stable enough to be fully characterized. Iridium(I) complexes such as *trans*-IrCl(CO)-$(PPh_3)_2$ (Vaska's complex) and its phosphine and halide derivatives have been employed as model starting materials for elucidating substrate reactivity by examination of the products formed during oxidative addition, reductive elimination, adduct formation, and migratory insertion reactions.[21−30] Variations

[⊗] Abstract published in *Advance ACS Abstracts*, March 1, 1995.

(1) Cotton, F. A.; Wilkinson, G. *Advanced Inorganic Chemistry*, 5th ed.; John Wiley and Sons, Inc.: New York, 1988.
(2) Collman, J. P.; Hegedus, L. S.; Norton, J. R.; Finke, R. G. *Principles and Applications of Organotransition Metal Chemistry*; University Science Books: Mill Valley, CA, 1987.
(3) Halpern, J.; Wong, C. S. *J. Chem. Soc., Chem. Commun.* **1973**, 629−630.
(4) Halpern, J.; Okamoto, T.; Zakhariev, A. *J. Mol. Catal.* **1976**, *2*, 65−68.
(5) Crabtree, R. *Acc. Chem. Res.* **1979**, *12*, 331−337.
(6) Crabtree, R. H.; Davis, M. W. *Organometallics* **1983**, *2*, 681−682.
(7) Stork, G.; Kahne, D. E. *J. Am. Chem. Soc.* **1983**, *105*, 1072−1073.
(8) Brown, J. M.; Hall, S. A. *Tetrahedron Lett.* **1984**, *25*, 1393−1396.
(9) Brown, J. M.; Naik, R. G. *J. Chem. Soc., Chem. Commun.* **1982**, 348−350.
(10) Brown, J. M.; Evans, P. L.; Lucy, A. R. *J. Chem. Soc., Perkin Trans. II* **1987**, 1589−1596.
(11) Evans, D. A.; Morrissey, M. M. *J. Am. Chem. Soc.* **1984**, *106*, 3866−3868.
(12) Schrock, R. R.; Osborn, J. A. *J. Am. Chem. Soc.* **1976**, *98*, 2143−2147.
(13) Schrock, R. R.; Osborn, J. A. *J. Am. Chem. Soc.* **1976**, *98*, 4450−4455.
(14) Bosnich, B.; Fryzuk, M. D. In *Topics in Inorganic and Organometallic Chemistry*; Geoffroy, G. L., Ed.; John Wiley and Sons: New York, 1981; Vol. 12, p 119.
(15) Bosnich, B. *Chem. Br.* **1984**, 808−811.
(16) Kagan, H. B.; Fiaud, J. C. In *Topics in Stereochemistry*; Eliel, E. L., Allinger, N. L., Eds.; John Wiley and Sons: New York, 1978; Vol. 10, p 175.
(17) Hayashi, T.; Kumada, M. *Acc. Chem. Res.* **1982**, *15*, 395−401.
(18) Vidal, J. L.; Walker, W. E. *Inorg. Chem.* **1981**, *20*, 249−261.
(19) Brown, C. K.; Wilkinson, G. *J. Chem. Soc. A* **1970**, 2753−2764.
(20) Yagupsky, G.; Brown, C. K.; Wilkinson, G. *J. Chem. Soc. A* **1970**, 1392−1401.
(21) Vaska, L.; DiLuzio, J. W. *J. Am. Chem. Soc.* **1961**, *83*, 2784−2785.
(22) Vaska, L.; DiLuzio, J. W. *J. Am. Chem. Soc.* **1962**, *84*, 679−680.
(23) Vaska, L. *Science* **1963**, *140*, 809−810.
(24) Vaska, L. *Acc. Chem. Res.* **1968**, *1*, 335−344.
(25) Vaska, L. *Acc. Chem. Res.* **1976**, *9*, 175−183.
(26) Halpern, J. *Acc. Chem. Res.* **1970**, *3*, 386−392.
(27) Blake, D. M.; Kubota, M. *Inorg. Chem.* **1970**, *9*, 989−991.
(28) Kubota, M.; Blake, D. M. *J. Am. Chem. Soc.* **1971**, *93*, 1368−1373.
(29) Collman, J. P.; Kang, J. W. *J. Am. Chem. Soc.* **1967**, *89*, 844−851.
(30) Chock, P. B.; Halpern, J. *J. Am. Chem. Soc.* **1966**, *88*, 3511−3514.

0002-7863/95/1517-3510$09.00/0 © 1995 American Chemical Society

of these iridium(I) complexes having alkyl, aryl, and alkoxy ligands in place of halide have been investigated as well, and they are interesting because they resemble some of the intermediates proposed to form during catalytic processes mentioned above.[31-43]

From our laboratory, studies have employed the di(phosphine) complex IrX(CO)(dppe) (X = Cl, Br, I, CN, H; dppe = 1,2-bis(diphenylphosphino)ethane), where the phosphine donors are necessarily cis, to examine and establish the stereoselectivity and kinetic control of H_2, Si–H, and H–X oxidative addition.[44-47] The formation of the stable complex $Ir(C_2H_5)(\eta^2\text{-}C_2H_4)(CO)$-(dppe), formed from the reaction of $IrH_3(CO)(dppe)$ and ethylene, promoted the search for an isolable four-coordinate alkyl or aryl derivative of IrX(CO)(dppe).[48] Herein we report the synthesis, structure, and reaction chemistry of the Ir(I) carbonyl dppe complex containing a σ-mesityl ligand, Ir(CO)-(mes)(dppe). This *cis*-phosphine aryl derivative of Vaska's complex undergoes oxidative addition reactions with C–H, Si–H, H_2, I_2, and H–Cl bonds, readily binds CO and carbonylates the coordinated aryl ligand, and in the presence of ethylene undergoes an unusual aryl to benzyl transformation. Part of this work has appeared in preliminary form.[49]

Results and Discussion

Formation of Ir(CO)(mes)(dppe) (1). The complex Ir(CO)-(mes)(dppe), **1**, is obtained by treating a tetrahydrofuran solution of IrBr(CO)(dppe)[44] with 2 equiv of (1,3,5-trimethylphenyl)-magnesium bromide (mesitylmagnesium bromide) at 0 °C under N_2 as shown in eq 1. After neutralization of excess Grignard reagent, the product is isolated and recrystallized from EtOH/Et_2O in 69% yield as orange, air-stable microcrystals.

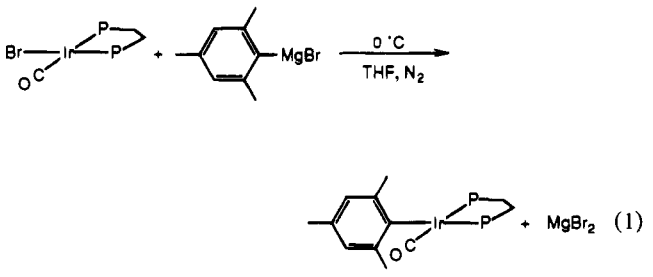

(1)

1

Complex **1** has been characterized spectroscopically, by microanalysis, and by single-crystal X-ray diffraction. Tables 1 and 2 contain a complete listing of spectroscopic data for **1** and all new compounds. The solution infrared spectrum of **1** in benzene exhibits a single ν_{CO} at 1968 cm^{-1}, indicative of terminal CO bound to Ir(I), while the $^{31}P\{^1H\}$ NMR spectrum of **1** shows two doublets at 49.06 and 46.52 ppm ($^2J_{P-P}$ = 9.7 Hz), consistent with two inequivalent, cis-coordinated phosphorus nuclei. In the ^1H NMR spectrum the *o*- and *p*-methyl groups of the mesityl ligand are seen as singlets at 2.50 and 2.36 ppm in a 6:3 intensity ratio, while the dppe methylene protons appear as two multiplets at 1.81 and 2.00 ppm. For the aromatic protons, two sets of dppe *o*-phenyl protons resonate at 7.80 and 7.26 ppm, while the dppe *m*- and *p*-phenyl protons, as well as the mesityl meta protons, exhibit overlapping signals between 7.09 and 6.86 ppm. From these results, **1** is assigned as a four-coordinate Ir(I) complex containing a σ-bound mesityl ligand.

While aryl and alkyl derivatives of Vaska's complex are well known, the vast majority of these Ir(I) systems have *trans*-phosphine arrangements.[31-43] Mixtures of cis and trans isomers of $Ir(R_nC_6H_{5-n})(CO)L_2$ ($R_nC_6H_{5-n}$ = 1,3,5-$Me_3C_6H_3$; 2,6-$Et_2C_6H_3$; 2-Et-6-MeC_6H_3; L = PPh_3, $PMePh_2$), however, have been reported to form by the reaction of $IrCl(CO)L_2$ with the appropriate aryllithium reagent.[50-52] In the present case, only one isomer of **1** having *cis*-phosphine donors is produced due to the geometric constraint imposed by the dppe ligand.

The structure determination of **1** using crystals grown from slow evaporation of a saturated toluene solution at −35 °C confirms the above assignment and is illustrated in Figure 1. A listing of cystallographic data, intramolecular bond angles, and intramolecular bond distances for **1** are presented in Tables 3, 4 and 5, respectively. The Ir–mesityl C bond length of 2.12-(1) Å is consistent with that of other iridium(I) mesityl complexes.[53] The four-coordinate complex deviates from ideal square planar geometry as shown by the bond angles of P1–Ir–P2, 83.0(1)°; P1–Ir–C25, 167.8(3)°; and P2–Ir–C34, 164.0(4)° and a dihedral angle of 18.2° between the planes defined by P1–Ir–P2 and C25–Ir–C34, indicative of slight tetrahedral distortion. These deviations apparently reduce the steric interactions between the dppe phenyl rings on P2 and the *o*-methyl groups of the coordinated mesityl ligand. A similar distortion of 23° was observed in *cis*-Ir(mes)(CO)$(PPh_3)_2$.[53] The two *o*-methyl groups C31 and C32 are 3.44 and 3.21 Å, respectively, from iridium and effectively shield both open faces of the Ir(I) complex. A close nonbonded contact of 2.19 Å is calculated between H28 on the *o*-mesityl methyl carbon C32 and iridium, which may facilitate the unusual reactivity described below.

Reaction of Ir(mes)(CO)(dppe) with Ethylene. Formation of $Ir(\eta^2\text{-}C_2H_4)(CH_2C_6H_3(CH_3)_2)(CO)$(dppe) (2). At ambient temperature, a benzene solution of **1** is unreactive with ethylene (2 atm), but when heated to 90 °C for 7 days, **1** undergoes an unusual transformation leading to the formation of the red-orange product **2**, in nearly quantitative yield (eq 2).

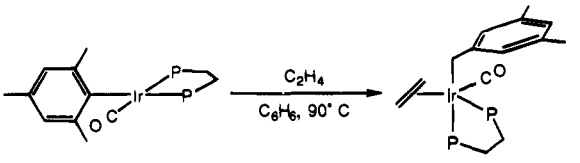

(2)

1 **2**

Complex **2** is identified by NMR and IR spectroscopies. The $^{31}P\{^1H\}$ NMR spectrum shows evidence of two inequivalent

(31) Schwartz, J.; Cannon, J. B. *J. Am. Chem. Soc.* **1972**, *94*, 6226–6229.
(32) Rausch, M. D.; Moser, G. A. *Inorg. Chem.* **1974**, *13*, 11–13.
(33) Rees, W. M.; Churchill, M. R.; Li, Y.-J.; Atwood, J. D. *Organometallics* **1985**, *4*, 1162–1167.
(34) Bernard, K. A.; Atwood, J. D. *Organometallics* **1989**, *8*, 795–800.
(35) Dahlenburg, L.; Nast, R. *J. Organomet. Chem.* **1976**, *110*, 395–406.
(36) Thompson, J. S.; Bernard, K. A.; Rappoli, B. J.; Atwood, J. D. *Organometallics* **1990**, *9*, 2727–2731.
(37) Rees, W. M.; Churchill, M. R.; Fettinger, J. C.; Atwood, J. D. *Organometallics* **1985**, *4*, 2179–2185.
(38) Rappoli, B. J.; Janik, T. S.; Churchill, M. R.; Thompson, J. S.; Atwood, J. D. *Organometallics* **1988**, *7*, 1939–1944.
(39) Rappoli, B. J.; McFarland, J. M.; Thompson, J. S.; Atwood, J. D. *J. Coord. Chem.* **1990**, *21*, 147–154.
(40) Thompson, J. S.; Randall, S. L.; Atwood, J. D. *Organometallics* **1991**, *10*, 3906–3910.
(41) Thompson, J. S.; Atwood, J. D. *Organometallics* **1991**, *10*, 3525–3529.
(42) Dahlenburg, L.; Nast, R. *J. Organomet. Chem.* **1974**, *71*, C49–C51.
(43) Dahlenburg, L.; Mirzaei, F.; Yardimcioglu, A. Z. *Naturforsch.* **1982**, *37b*, 310–317.
(44) Johnson, C. E.; Fisher, B. J.; Eisenberg, R. *J. Am. Chem. Soc.* **1983**, *105*, 7772–7774.
(45) Johnson, C. E.; Eisenberg, R. *J. Am. Chem. Soc.* **1985**, *107*, 3148–3160.
(46) Johnson, C. E.; Eisenberg, R. *J. Am. Chem. Soc.* **1985**, *107*, 6531–6540.

Table 1. ^{1}H NMR Spectroscopic Data for Complexes **1**−**12**[a]

complex	δ dppe	δ R	δ H
Ir(mes)(CO)(dppe) (**1**)	7.80; dd; 4H; *o*-Ph	2.50; s; 6H; *o*-CH_3	
	7.26; dd; 4H; *o*-Ph	2.36; s; 3H; *p*-CH_3	
	7.09−6.86; m; *m*, *p*-Ph[b]		
	2.00; m; 2H		
	1.81; m; 2H		
Ir(η^2-C_2H_4)($CH_2C_6H_3(CH_3)_2$)(CO)(dppe) (**2**)	7.70; m; 2H; *o*-Ph	7.18−7.00; *o*-3,5-DMB[d]	
	7.55; m; 2H; *o*-Ph	6.61; s; 1H; *p*-3,5-DMB	
	7.45; m; 2H; *o*-Ph	3.15; m; 1H; benzylic	
	7.18−7.00; *o*-Ph[c]	2.20; s; 6H; -CH_3	
	6.91; *m*, *p*-Ph	2.11; m; 1H; η^2-C_2H_4	
	2.24; m; 1H	1.99; m; 1H; η^2-C_2H_4	
	2.11; m; 1H	1.50; m; 1H; benzylic	
	1.99; m; 1H	0.98; m; 1H; η^2-C_2H_4	
	1.72; m; 1H	0.79; m; 1H; η^2-C_2H_4	
Ir(C_6F_6)(CO)(dppe) (**3**)	7.68; dd; 4H; *o*-Ph		
	7.32; m; 4H; *o*-Ph		
	7.04−6.98; m; *m*, *p*-Ph		
	1.83; m; 4H		
Ir(*o*-tolyl)(CO)(dppe) (**4**)	7.76; dd; 4H; *o*-Ph	7.88; t; 1H; *p*-Ph	
	7.33; dd; 4H; *o*-Ph	7.12−6.80; m; *m*, *o*-Ph	
	7.12−6.80; *m*, *p*-Ph[c]	2.49; s; 3H; *o*-CH_3	
	2.04; m; 2H		
	1.80; m; 2H		
Ir(benzyl)(CO)(dppe) (**5**)	7.55; m; 4H; *o*-Ph	7.15; t; 1H; *p*-Ph	
	7.43; m; 4H; *o*-Ph	7.11−6.88; m; *m*, *o*-Ph	
	7.11−6.88; m; *p*, *m*-Ph[c]	3.84; dd; $^3J_{H-P}$ = 8.4, 7.4 Hz;	
	1.87; m; 4H	2H; benzylic	
3 + ethylene	7.95; broad s; 4H; *o*-Ph	2.66−1.38; broad m; 3H	
	7.57−6.45; broad m; *p*, *o*, *m*-Ph	0.95; broad m; 1H	
	2.66−1.38; broad m; 4H		
4 + ethylene	7.84; broad s; 2H; *o*-Ph	7.26; d; *o*-Ph	
	7.72; broad s; 4H; *o*-Ph	7.20−6.69; broad m; *p*, *m*-Ph	
	7.55; broad s; 2H; *o*-Ph	3.17; s; 3H; -CH_3	
	7.20−6.69; broad m; *p*, *m*-Ph[c]	2.50; broad m; 1H; η^2-C_2H_4	
	2.21; broad m; 2H	2.21; broad m; 1H; η^2-C_2H_4	
	1.85; broad m; 2H	1.59; broad m; 1H; η^2-C_2H_4	
		1.28; broad m; 1H; η^2-C_2H_4	
5 + ethylene	7.73; dd; 2H; *o*-Ph	7.31−6.83; m; *o*, *p*, *m*-Ph	
	7.56; dd; 2H; *o*-Ph	3.25; m; 1H; benzylic	
	7.46; dd; 2H; *o*-Ph	2.23; m; 1H; η^2-C_2H_4	
	7.31−6.83; m; *o*, *p*, *m*-Ph[c]	1.74; m; 1H; η^2-C_2H_4	
	2.09; m; 2H	1.00; m; 1H; η^2-C_2H_4	
	2.01; m; 2H	0.80; m; 1H; η^2-C_2H_4	
$Ir(CO)_2(C(O)C_6H_2(CH_3)_3)$(dppe) (**6**)[e]	7.69; m; 4H; *o*-Ph	6.58; s; 2H	
	7.49; m; 4H; *o*-Ph	2.17; s; 3H; *p*-CH_3	
	7.43; br. s; 12H; *m*, *p*-Ph	1.75; s; 6H; *o*-CH_3	
	2.49; m; 2H		
	2.29; m; 2H		
trans-IrH(CO)($CH_2C_6H_2(CH_3)_2C(O)$)(dppe) (**7**)	8.07; dd; 2H; *o*-Ph	7.29; s; 1H; Ph	−7.98; t; $^2J_{H-P}$ = 19 Hz; 1H
	7.61; dd; 2H; *o*-Ph	6.64; s; 1H; Ph	
	7.42; dd; 4H; *o*-Ph	3.77; AB q; 2H; benzylic	
	7.15−6.65; m; *p*, *m*-Ph	2.92; s; 3H; CH_3	
	2.15; m; 2H	2.13; s; 3H; CH_3	
	1.86; m; 2H		
cis-IrH(CO)($CH_2C_6H_2(CH_3)_2C(O)$)(dppe) (**8**)	8.17; dd; 2H; *o*-Ph	6.45; s; 1H; Ph	−8.01; ddd; $^2J_{H-P}$ = 136, 13 Hz;
	7.91; dd; 2H; *o*-Ph	6.30; s; 1H; Ph	$^2J_{H-H}$ = 2 Hz; 1H
	7.69; dd; 2H; *o*-Ph	3.00; s; 3H; CH_3	
	7.37; dd; 2H; *o*-Ph	2.85; m; 1H; benzylic	
	7.15−6.65; m; *p*, *m*-Ph	1.90; s; 3H; CH_3	
	2.70; m; 1H	1.50; dt; $^3J_{H-P}$ = 16,	
		$^3J_{H-H}$ = 2 Hz; benzylic	
	2.15; m; 2H		
	1.86; m; 1H		
$IrH(SiHPh_2)(CO)$(mes)(dppe) (**9**)[f]	1.92; m; 4H[g]	5.76; m; 1H; Si-H	−8.42; t; $^2J_{H-P}$ = 18.8 Hz; 1H
		2.46; s; 3H; CH_3	
		2.25; s; 3H; CH_3	
		2.12; s; 3H; CH_3	
$IrH_2(CO)$(mes)(dppe) (**10**)[h]	8.00; m; 2H; *o*-Ph	6.66; s; 2H	−9.93; dd; $^2J_{H-P}$ =
	7.58; m; 2H; *o*-Ph	2.26; s; 6H; *o*-CH_3	132.0, 12.9 Hz; 1H
	7.42; m; 12H; *p*, *m*-Ph	2.11; s; *p*-CH_3	−10.06; dd; $^2J_{H-P}$ =
	7.26; m; 2H; *o*-Ph		28.0, 18.8 Hz, 1H

Table 1. Continued

complex	δ dppe	δ R	δ H
	7.14; m; 2H; *o*-Ph		
	2.65; m; 2H		
	2.11; m		
$IrI_2(C(O)C_6H_2(CH_3)_3)(dppe)$ (**11**)[g]	7.93; dd; 4H; *o*-Ph	6.25; s; 2H	
	7.63; dd; 4H; *o*-Ph	2.02; s; 3H; *p*-CH_3	
	7.53; m; 2H; *p*-Ph	1.01; s; 6H; *o*-CH_3	
	7.46; dd, 4H; *m*-Ph		
	7.40; dd; 2H; *p*-Ph		
	7.28; dd; 4H; *m*-Ph		
	3.40; m; 2H		
	2.06; m; 2H		
$IrHCl_2(CO)(dppe)$ (**12**)[g]	7.79; m; 4H; *o*-Ph		−16.73; dd; $^2J_{H-P}$ = 14.0; 11.7 Hz; 1H
	7.58; m; 4H; *o*-Ph		
	7.47; m; 12H; *p*, *m*-Ph		
	3.18; m; 1H		
	2.95; m; 1H		
	2.62; m; 1H		
	2.17; m; 1H		

[a] All spectra are reported in ppm downfield relative to tetramethylsilane in benzene-d_6 unless noted otherwise. [b] The *m*, *p*-Ph resonances overlap with the *m*-mesityl resonances. [c] The dppe phenyl resonances overlap with those of the σ-benzyl or σ-aryl resonances. [d] DMB = dimethylbenzyl. [e] Spectrum obtained at 250 K in methylene chloride-d_2. [f] Spectrum obtained in methylene chloride-d_2. [g] Due to overlapping phenyl resonances, not all resonances are assigned. Refer to Experimental Section for aromatic peak listings. [h] Spectrum obtained in methylene chloride-d_2 at 253 K.

Table 2. IR, $^{31}P\{^1H\}$ NMR, and $^{13}C\{^1H\}$ NMR Spectroscopic Data for Complexes **1**−**12**[a]

complex	IR (cm^{-1})[b]	δ P; multiplicty	$^2J_{P-P}$ (Hz)	δ C; multiplicity[c]	$^2J_{C-P}$ (Hz)
Ir(mes)(CO)(dppe) (**1**)	1968	49.06; d	9.7	189.66; dd	112, 9
		46.52; d			
Ir(η^2-C_2H_4)($CH_2C_6H_3(CH_3)_2$)(CO)(dppe) (**2**)	1955[d]	28.1; d	5.0	184.8; d	17
		21.9; d		8.3; dd; benzylic	72, 6
Ir(C_6F_6)(CO)(dppe) (**3**)	1980[e]	49.88; d	13.9	187.05; dd	110, 10
		48.33; m			
Ir(*o*-tolyl)(CO)(dppe) (**4**)	1969	50.43; d	10.0		
		48.41; d			
Ir(benzyl)(CO)(dppe) (**5**)	1959	52.25; d	8.3		
		51.15; d			
3 + ethylene		28.83; sept			
		15.43; t			
4 + ethylene		23.04; broad s			
		16.67; broad s			
5 + ethylene		28.47; d	2.8		
		28.00; d			
Ir(CO)$_2$(C(O)$C_6H_2(CH_3)_3$)(dppe) (**6**)	1986[f]	25.2; d[g]	6.0	221.5; d; acyl[g]	66
	1935	20.3; d		186.9; d	23
	1601				
trans-IrH(CO)($CH_2C_6H_2(CH_3)_2$C(O))(dppe) (**7**)	2076; ν_{Ir-H}	17.69; AB q	18.7	225.2; dd; acyl	93, 9
	2017			178.8; t	4
	1607; acyl			2.81; d; benzylic	55
cis-IrH(CO)($CH_2C_6H_2(CH_3)_2$C(O))(dppe) (**8**)	2076; ν_{Ir-H}	21.06; d	5.0	228.6; dd; acyl	91, 7
	2017	15.52; d		174.9; t	4
	1607; acyl			11.2; s; benzylic	
IrH($SiHPh_2$)(CO)(mes)(dppe) (**9**)	2173; ν_{Si-H}[e]	22.7; d	3.1	180.7; t	4
	2048; ν_{Ir-H}	15.4; d			
	1968				
IrH_2(CO)(mes)(dppe) (**10**)		27.5; d[h]	7.2	178.9; t	4
		17.5; d			
$IrI_2(C(O)C_6H_2(CH_3)_3)$(dppe) (**11**)	1664[e]	16.85; s[i]			
$IrHCl_2$(CO)(dppe) (**12**)	2214; ν_{Ir-H}[f]	14.58; d	7.3	169.0; dd	139, 7
	2075	7.24; d			

[a] $^{31}P\{^1H\}$ NMR spectra are reported downfield of external 85% phosphoric acid. $^{13}C\{^1H\}$ NMR spectra are reported downfield of tetramethylsilane and are referenced to a known carbon signal in the solvent. All spectra are recorded in benzene-d_6 unless noted otherwise. [b] All IR spectra are recorded in benzene unless noted otherwise. ν_{CO} listed, other assignments noted. [c] Terminal carbonyl listed, other assignments noted. [d] Spectrum obtained in benzene-d_6. [e] Spectrum obtained as a KBr mull. [f] Spectrum obtained in methylene chloride. [g] Spectrum obtained in methylene chloride-d_2 at 250 K. [h] Spectrum obtained in methylene chloride-d_2 at 253 K. [i] Spectrum obtained in methylene chloride-d_2.

cis-phosphine donors at 28.1 and 21.9 ppm ($^2J_{P-P}$ = 5.0 Hz) while a ν_{CO} of 1955 cm^{-1} establishes terminal CO coordination to Ir(I). The ^1H NMR spectrum exhibits a single methyl resonance and resonances (see Table 1) assignable to two diastereotopic benzylic protons. The results thus indicate that the mesityl ligand has been transformed into a 3,5-dimethylbenzyl ligand via a process requiring methyl C−H bond activation. On the basis of the ^1H NMR spectrum of the previously reported ethyl−ethylene complex, Ir(C_2H_5)(C_2H_4)(CO)(dppe), which shows an upfield shift of coordinated ethylene resonances and through the application of a COSY ^1H NMR experiment, we are able to discriminate the four dppe methylene signals from overlapping ethylene resonances. The solution structure of **2** contains a static (on the NMR time scale) ethylene ligand since each of its four protons are observed and appear highly coupled. The $^{13}C\{^1H\}$ 135° DEPT spectrum

Table 3. Summary of Crystallographic Data for Complexes **1**, **2**, and **8**

	1	**2**	**8**
empirical formula	$C_{36}H_{35}IrOP_2$	$C_{39}H_{40}IrO_{1.5}P_2$	$C_{37}H_{35}IrO_2P_2$
crystal system	monoclinic	orthorhombic	monoclinic
space group	$P2_1/n$ (No. 14)	*Pbca* (No. 61)	$P2_1/n$ (No. 14)
Z	4	8	4
a, Å	8.953(3)	19.113(8)	10.701(3)
b, Å	22.752(6)	16.243(9)	14.554(3)
c, Å	16.212(6)	23.174(7)	20.760(6)
β, deg	99.00(3)		90.19(3)
V, Å^3	3259(3)	7194(9)	3233(3)
d_{calc}, g/cm^3	1.503	1.463	1.573
T, °C	0	0	0
diffractometer	Enraf-Nonius CAD4	Enraf-Nonius CAD4	Enraf-Nonius CAD4
$\lambda_{Mo\ K\alpha}$ (graphite monochromated)	0.71069	0.71069	0.71069
scan type	$\omega/2\theta$	$\omega/2\theta$	$\omega/2\theta$
scan rate, deg/min	2−16.5	2−16.5	2−16.5
total background time	scan time/2	scan time/2	scan time/2
take-off angle, deg	2.6	2.6	2.6
scan range, deg	$0.8 + 0.35 \tan \theta$	$0.8 + 0.35 \tan \theta$	$0.8 + 0.35 \tan \theta$
2θ range, deg	4−44	4−44	4−50
data collected	$+h,+k,\pm l$	$+h,+k,+l$	$+h,+k,\pm l$
no. of data collected	4438	4890	6459
no. of unique data > 3σ	2545	2667	4050
no. of parameters varied	361	391	379
absorption coefficient, cm^{-1}	42.031	38.144	42.419
systematic absences	$h0l$, l odd; $0k0$, k odd	$h0l$, l odd; $0k0$, k odd, $00l$, l odd	$h0l$, l odd; $0k0$, k odd
absorption correction	differential	differential	differential
range of transmission factors	0.904−1.164	0.862−1.191	0.904−1.164
equivalent data	$0kl$, $0\bar{k}l$		$0kl$, $0\bar{k}l$
agreement of equivalent data (F_o)	0.056		0.036
R	0.032	0.034	0.029
R_w	0.033	0.038	0.032
goodness of fit	1.122	1.299	1.187
largest positive peak in final e-map	0.467	0.651	0.581
largest negative peak in final e-map	−0.474	−0.408	−0.768

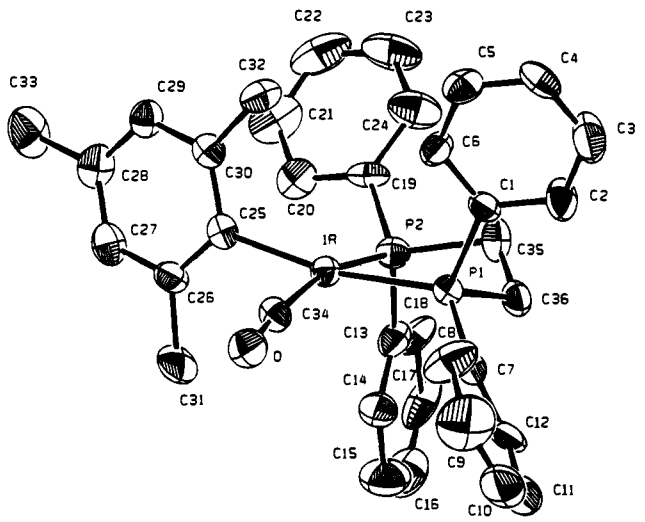

Figure 1. ORTEP plot of Ir(CO)(mes)(dppe), **1**. Thermal ellipsoids are shown at 35% probability.

confirms the presence of the benzylic carbon as an inverted doublet of doublets ($^2J_{C-P}$ = 72, 6 Hz) at 8.3 ppm, but the ^{13}C chemical shifts of the coordinated ethylene, which would provide a measure of the amount of metal-to-olefin π-back bonding, were not determined.[54] On the basis of the spectroscopic data, **2** is assigned as Ir(η^2-C_2H_4)($CH_2C_6H_3(CH_3)_2$)(CO)(dppe), which has experienced an unusual aryl to benzyl transformation. Other related alkyl olefin complexes of Ir(I) include the above-cited Ir(Et)(η^2-C_2H_4)(CO)(dppe) derivative, Bianchini's Ir(Et)(η^2-C_2H_4)(triphos) complex (triphos = 1,1,1-tris((diphenylphosphi-

Table 4. Selected Intramolecular Bond Angles (deg) for Ir(mes)(CO)(dppe) (**1**)

atoms	angle	atoms	angle
P1−Ir−P2	83.0(1)	C26−C25−C30	117(1)
P1−Ir−C25	167.8(3)	C25−C26−C27	121(1)
P1−Ir−C34	95.1(4)	C25−C26−C31	123(1)
P2−Ir−C25	89.8(3)	C27−C26−C31	116(1)
P2−Ir−C34	164.0(4)	C26−C27−C28	122(1)
C25−Ir−C34	94.5(4)	C27−C28−C29	118(1)
Ir−P1−C1	113.6(4)	C27−C28−C33	121(1)
Ir−P1−C7	122.7(4)	C29−C28−C33	121(1)
Ir−P1−C36	110.0(4)	C28−C29−C30	121(1)
Ir−P2−C13	112.3(4)	C25−C30−C29	121(1)
Ir−P2−C19	122.4(4)	C25−C30−C32	121(1)
Ir−P2−C35	107.9(4)	C29−C30−C32	118(1)
Ir−C25−C26	125(1)	Ir−C34−O	173(1)
Ir−C25−C30	117.6(8)		

Table 5. Selected Intramolecular Bond Distances (Å) for Ir(mes)(CO)(dppe) (1)

atoms	distance	atoms	distance
Ir−P1	2.280(3)	C26−C27	1.41(1)
Ir−P2	2.328(3)	C26−C31	1.51(2)
Ir−C25	2.12(1)	C27−C28	1.36(2)
Ir−C34	1.84(1)	C28−C29	1.38(2)
O−C34	1.13(1)	C28−C33	1.52(1)
C25−C26	1.37(1)	C29−C30	1.39(1)
C25−C30	1.41(1)	C30−C32	1.50(1)

(47) Hays, M. K.; Eisenberg, R. *Inorg. Chem.* **1991**, *30*, 2623−2630.
(48) Deutsch, P. P.; Eisenberg, R. *J. Am. Chem. Soc.* **1990**, *112*, 714−721.
(49) Cleary, B. P.; Eisenberg, R. *Organometallics* **1992**, *11*, 2335−2337.
(50) Dahlenburg, L.; Von Deuten, K.; Kopf, J. *J. Organomet. Chem.* **1981**, *216*, 113−127.
(51) Dahlenburg, L.; Nast, R. *Angew. Chem., Int. Ed. Engl.* **1976**, *15*, 110−111.
(52) Mirzaei, F.; Dahlenburg, L. *J. Organomet. Chem.* **1979**, *173*, 325−333.
(53) Dahlenburg, L.; Mirzaei, F. *J. Organomet. Chem.* **1983**, *251*, 113−122.

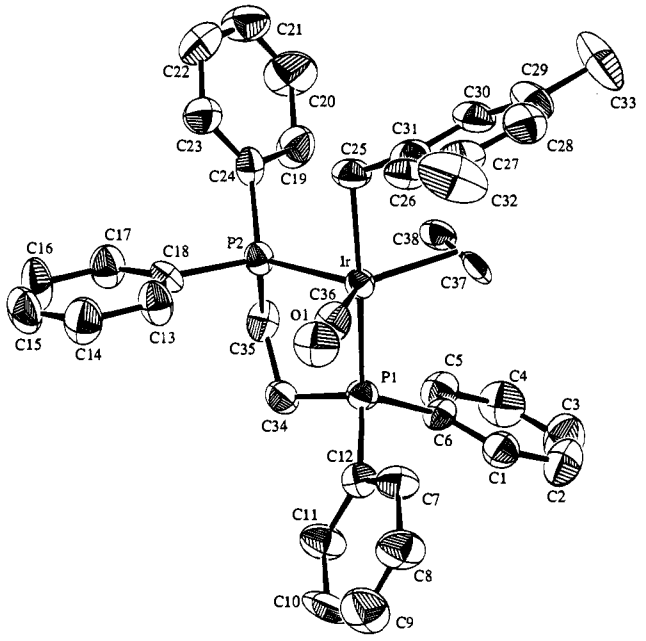

Figure 2. ORTEP plot of $Ir(\eta^2\text{-}C_2H_4)(CH_2C_6H_3(CH_3)_2)(CO)(dppe)\cdot{}^1/_2C_2H_5OH$. Thermal ellipsoids shown at 50% probability.

Table 6. Selected Intramolecular Bond Angles (deg) for $Ir(\eta^2\text{-}C_2H_4)(CH_2C_6H_3(CH_3)_2)(CO)(dppe)\cdot{}^1/_2C_2H_5OH$

atoms	angle	atoms	angle
P1–Ir–P2	84.9(1)	Ir–P2–C24	118.8(3)
P1–Ir–C25	174.2(3)	Ir–P2–C35	106.7(3)
P1–Ir–C36	96.8(4)	Ir–C25–C31	115.3(7)
P1–Ir–C37	91.9(3)	C27–C26–C31	122(1)
P1–Ir–C38	91.9(3)	C26–C27–C28	119(1)
P2–Ir–C25	89.8(3)	C26–C27–C32	121(1)
P2–Ir–C36	111.3(4)	C28–C27–C32	120(1)
P2–Ir–C37	133.8(3)	C27–C28–C29	122(1)
P2–Ir–C38	95.6(3)	C28–C29–C30	117(1)
C25–Ir–C36	87.3(5)	C28–C29–C33	123(1)
C25–Ir–C37	90.0(4)	C30–C29–C33	120(1)
C25–Ir–C38	86.2(4)	C29–C30–C31	124(1)
C36–Ir–C37	114.9(5)	C25–C31–C26	122(1)
C36–Ir–C38	152.3(5)	C25–C31–C30	121(1)
C37–Ir–C38	38.4(4)	C26–C31–C30	117(1)
Ir–P1–C6	119.1(3)	Ir–C36–O1	178(1)
Ir–P1–C12	118.0(4)	Ir–C37–C38	69.8(6)
Ir–P1–C34	107.8(4)	Ir–C38–C37	71.8(6)
Ir–P2–C18	120.8(4)		

no)methyl)ethane), $Ir(CH_3)(CO)(PPh_3)_2(CH_3CO_2CH{=}CHCO_2CH_3)$, $Ir(\eta^4\text{-diene})_2R$ (R = Bz, c-C_3H_5), and $Ir(CH_3CHCN)(CH_2{=}CHCN)(CO)(PPh_3)_2$.[48,55-58]

The structure of **2** was further elucidated by an X-ray diffraction study and is shown in Figure 2. Complex **2** is the first structural example of both an iridium(I) benzyl complex and a benzyl ethylene complex containing a platinum group metal. A listing of cystallographic data, intramolecular bond angles, and intramolecular bond distances for **2** are presented in Tables 3, 6, and 7, respectively. The solid state geometry of **2** is best described as a distorted trigonal bipyramid with dppe spanning axial and equatorial sites, the 3,5-dimethylbenzyl ligand resident in the other axial position, and CO and η^2-C_2H_4 ligands occupying the remaining equatorial sites. The equatorial bond angles of P2–Ir–C36, P2–Ir–(C37–C38)$_{center}$, and C36–Ir–(C37–C38)$_{center}$ (111.4(4), 114.8, and 133.6°, respectively) and the trans axial bond angle of C25–Ir–P1 (174.2(3)°) indicate slight distortion of **2** from the idealized trigonal bipyramidal geometry. The iridium–C25 bond of 2.21(1) Å is considerably longer than the two iridium(III)–benzyl bonds of 2.102(3) and 2.125(3) Å found in $Ir(CH_2C_6H_5)_2(N(SiMe_2CH_2PPh_2)_2)$.[59] The difference in the Ir–C(benzyl) bond lengths reflects the different oxidation states of iridium in the two complexes. The distances between iridium and the ethylene carbon atoms average 2.16 Å, which is similar to values of 2.168 Å in $Ir(C_2H_4)_2PPh_2C_6H_4PPh_3$, 2.150 Å in $Ir(C_2H_4)_2P\text{-}i\text{-}Pr_2C_3H_6P\text{-}i\text{-}Pr_3$, and 2.12 Å in *trans*-$IrCl(C_2H_4)(PPh_3)_2$.[60,61] The ethylene bond length of 1.42(1) Å is similar to that found in $Ir(C_2H_4)_2PPh_2C_6H_4PPh_3$ and $Ir(C_2H_4)_2P\text{-}i\text{-}Pr_2C_3H_6P\text{-}i\text{-}Pr_3$, 1.45 and 1.43 Å, respectively, but longer than the 1.375 Å value found in *trans*-$IrCl(C_2H_4)(PPh_3)_2$.[60,61] The coordinated ethylene C–C bond length in **2** is intermediate between that of C–C double and single bonds, indicating that the iridium–ethylene moiety possesses some metallacyclopropane character.[62]

Table 7. Selected Intramolecular Bond Distances (Å) for $Ir(\eta^2\text{-}C_2H_4)(CH_2C_6H_3(CH_3)_2)(CO)(dppe)\cdot{}^1/_2C_2H_5OH$

atoms	distance	atoms	distance
Ir–P1	2.319(3)	C26–C31	1.39(1)
Ir–P2	2.310(3)	C27–C28	1.40(2)
Ir–C25	2.21(1)	C27–C32	1.49(2)
Ir–C36	1.88(1)	C28–C29	1.38(2)
Ir–C37	2.17(1)	C29–C30	1.39(2)
Ir–C38	2.14(1)	C29–C33	1.52(2)
O1–C36	1.15(1)	C30–C31	1.40(1)
C25–C31	1.50(1)	C37–C38	1.42(1)
C26–C27	1.37(2)		

The rearrangement shown in eq 2 of a metal–aryl to a metal–benzyl moiety is unusual because the iridium–mesityl bond strength is presumed to be greater than that of an iridium–benzyl bond.[63] To the authors' knowledge, there are no other examples of this type of rearrangement.[64,65] A likely mechanism to account for the rearrangement of mesityl to 3,5-dimethylbenzyl is proposed to be by C–H oxidative addition of an *o*-mesityl methyl group to form the cyclometalated-hydride intermediate **A**, which then reductively eliminates the aryl C–H bond followed by ethylene coordination, as shown in Figure 3. The methyl C–H oxidative addition may be facilitated by a short nonbonding contact of 2.19 Å between H28 and the iridium(I) center found in **1**. In support of the proposed mechanism, Flood has determined that the formation of *fac*-$L_3Ir(H)(\eta^2CH_2EMe_2CH_2)$ (E = C, Si), which contains a similar four-membered metallocycle, proceeds via intramolecular ligand C–H oxidative addition.[65-68] While the proposed mechanism

(54) Tsutsui, M.; Levy, M. N.; Nakamura, A.; Ichikawa, M.; Mori, K. *Introduction to Metal π-Complex Chemistry*; Plenum Press: New York, 1970.
(55) Barbaro, P.; Bianchini, C.; Meli, A.; Peruzzini, M.; Vacca, A.; Vizza, F. *Organometallics* **1991**, *10*, 2227–2238.
(56) Churchill, M. J.; Fettinger, J. C.; Rees, W. M.; Atwood, J. D. *J. Organomet. Chem.* **1986**, *301*, 99–108.
(57) Müller, J.; Friedrich, C.; Gaede, P. E.; Sodemann, S.; Qiao, K. *J. Organomet. Chem.* **1994**, *471*, 249–258.
(58) Drouin, M.; Harrod, J. F. *Can. J. Chem.* **1985**, *63*, 353–360.
(59) Fryzuk, M. D.; MacNeil, P. A.; Massey, R. L.; Ball, R. G. *J. Organomet. Chem.* **1989**, *368*, 231–247.
(60) Restivo, R. J.; Ferguson, G.; Kelly, T. L.; Senoff, C. V. *J. Organomet. Chem.* **1975**, *90*, 101–109.
(61) Perego, G.; Del Piero, G.; Cesari, M.; Clerici, M. G.; Perrotti, E. *J. Organomet. Chem.* **1973**, *54*, C51–C52.
(62) Crabtree, R. H. *The Organometallic Chemistry of the Transition Metals*; John Wiley and Sons: New York, 1988.
(63) Martinho Simoes, J. A.; Beauchamp, J. L. *Chem. Rev.* **1990**, *90*, 629.
(64) Stella, S.; Chiang, M.; Floriani, C. *J. Chem. Soc., Chem. Commun.* **1987**, 161–163.
(65) Tulip, T. H.; Thorn, D. L. *J. Am. Chem. Soc.* **1981**, *103*, 2448–2450.
(66) Foley, P.; DiCosimo, R.; Whitesides, G. M. *J. Am. Chem. Soc.* **1980**, *102*, 6713–6725.
(67) Harper, T. G. P.; Desrosiers, P. J.; Flood, T. C. *Organometallics* **1990**, *9*, 2523–2528.
(68) Shinomoto, R. S.; Desrosiers, P. J.; Harper, G. P.; Flood, T. C. *J. Am. Chem. Soc.* **1990**, *112*, 704–713.

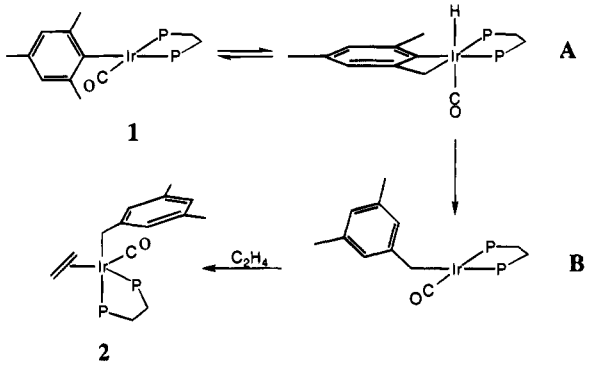

Figure 3. Proposed mechanism for the formation of $Ir(\eta^2\text{-}C_2H_4)(CH_2C_6H_3(CH_3)_2)(CO)(dppe)$, **2**.

has significant precedent, no intermediates are observed during the reaction when monitored by NMR spectroscopy.

The coordination of ethylene to **2** appears to be reversible based on the fact that reaction with H_2 yields the known Ir(III) complex $IrH_3(CO)(dppe)$ together with ethylene and mesitylene (eq 3). The formation of $IrH_3(CO)(dppe)$ is believed to occur via classical oxidative addition and reductive elimination reactions following the loss of ethylene from **2**.

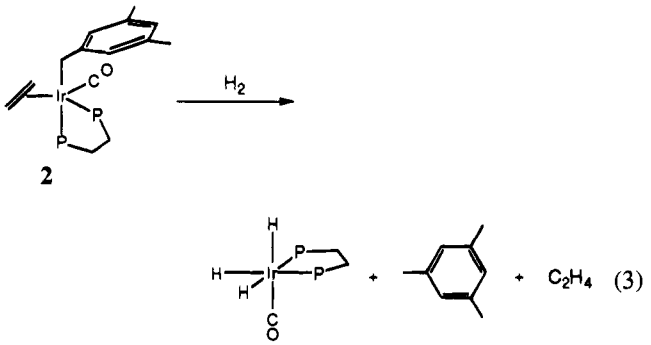

The fact that **1** does not react with ethylene at ambient temperature suggests that the incoming olefin is prevented from coordinating to iridium because of steric interactions with the *o*-methyl groups of the mesityl ligand. Once the methyl groups are distanced from the metal center via rearrangement, ethylene coordination is facile. Attempts to facilitate ethylene insertion into the benzyl–iridium bond at temperatures higher than 90 °C resulted in complex decomposition.

In light of the observation that the two methyl groups of the mesityl ligand prevent coordination of ethylene, other aryl and akyl derivatives of **1** were prepared including $Ir(C_6F_5)(CO)(dppe)$ (**3**), Ir(*o*-tolyl)(CO)(dppe) (**4**), and Ir(benzyl)(CO)(dppe) (**5**) to determine the influence of sterics on ethylene coordination. Benzene solutions of each compound immediately change color when placed under ethylene, indicating a reaction had occurred. ^1H NMR spectra (Tables 1 and 2) for room temperature reactions with **3** and **4** display broad resonances for coordinated and free ethylene, implying reversible adduct formation on the NMR time scale, while **5** displays four separate and highly coupled resonances, attributable to a static ethylene adduct. These results display the significance of the shielding effect imparted to the planar Ir(I) complex by the two *o*-methyl groups of the mesityl ligand.

Reaction of Ir(mes)(CO)(dppe) with CO. Formation of $Ir(CO)_2(C(O)C_6H_2(CH_3)_3)(dppe)$ (6). Under CO (1 atm) in C_6H_6 or CH_2Cl_2, complex **1** converts readily to the 2,4,6-trimethylbenzoyl complex $Ir(CO)_2(C(O)C_6H_2(CH_3)_3)(dppe)$ (**6**), which is characterized by IR and NMR spectroscopies and microanalyses (eq 4). The infrared spectrum displays two terminal CO bands at 1986 and 1935 cm^{-1} while an acyl absorption appears at 1601 cm^{-1}. Broad resonances are present for the dppe phenyl and methylene protons in the room temperature ^1H NMR spectrum of **6**, but they separate into sharp, distinct resonances when cooled below 282 K.

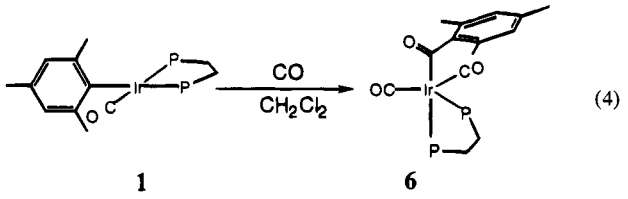

The coordination geometry of the dicarbonyl acyl complex **6** is most probably trigonal bipyramidal on the basis of the analogous propionyl complex $Ir(C(O)C_2H_5)(CO)_2(dppe)$,[69] which has been characterized structurally. In that structure, the acyl group occupies one of the axial positions of a trigonal bipyramid, the dppe ligand spans axial and equatorial sites, and the terminal carbonyls reside in the remaining equatorial positions. Spectroscopic data for **6** support this arrangement. The $^{13}C\{^1H\}$ NMR spectrum shows that the acyl carbonyl carbon nucleus has a $^2J_{C-P}$ coupling constant of 66 Hz, indicative of a *trans*-acylphosphine arrangement, while the intensities of the symmetric and asymmetric stretches of the terminal carbonyl ligands yield a calculated value of 123° between them on the basis of eq 5, where $I(sym)$ is the intensity of the symmetric mode, $I(asym)$ is the intensity of the asymmetric mode, and θ is the

$$\frac{I(\text{sym})}{I(\text{asym})} = \cot^2\theta \qquad (5)$$

carbonyl–Ir–carbonyl angle.[1,62]

The mechanism for the formation of **6** can be explained by a series of facile equilibria illustrated in Figure 4. Complex **1** coordinates CO to yield a five-coordinate dicarbonylmesityliridium(I) intermediate (**C**) that undergoes CO insertion followed by coordination of an additional CO to yield **6**. Allowing a degassed CD_2Cl_2 solution of **6** to react with 700 Torr of ^{13}CO explored the reversibility of the proposed mechanism. After 30 min at room temperature, the $^{31}P\{^1H\}$ NMR spectrum at 208 K shows that 50% of the trans axial phosphorus resonance is ^{13}CO acyl coupled ($^2J_{P-C}$ = 66 Hz) while the equatorial phosphorus resonance displays extreme broadening ($\omega_{1/2}$ = 62 Hz) due to additional unresolved *cis*-^{13}CO coupling. These results indicate that after 30 min of exposure to ^{13}CO, 50% of the acyl carbonyl is exchanged with ^{13}CO. A quantitative value of ^{13}CO incorporation into the equatorial sites was not possible due to the unresolved nature of the equatorial phosphorus resonance. The steps in the formation of **6** are similar in part to the mechanism proposed for the homogeneous hydroformylation of olefins catalyzed by $RhH(CO)(PPh_3)_2$ and provide another example of the utility of using a congeneric complex to model individual steps in a catalytic process.[19,20]

In contrast with **2**, complex **6** is fluxional above 264 K on the basis of equilibration of the dppe methylene protons and the phosphorus nuclei as shown by NMR spectroscopies. Figure 5 shows the variable temperature ^1H spectra for the aromatic signals, region A, and dppe methylene signals, region B, between 250 and 320 K. The fluxionality in **6** can be ascribed to either a pseudorotation or a turnstile process that serves to interconvert the axial and equatorial phosphorus atoms.[70–72]

(69) Deutsch, P. P.; Eisenberg, R. *Organometallics* **1990**, *9*, 709–718.
(70) Berry, R. S. *J. Chem. Phys.* **1960**, *32*, 933–938.
(71) Ugi, I.; Marquarding, D.; Klusacek, H.; Gillespie, P. *Acc. Chem. Res.* **1971**, *4*, 288–296.
(72) Musher, J. I. *J. Am. Chem. Soc.* **1972**, *94*, 5662–5665.

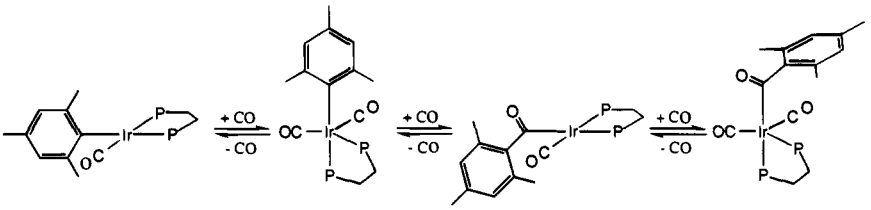

1 C D 6

Figure 4. Proposed mechanism for the formation of $Ir(CO)_2(C(O)C_6H_2(CH_3)_3)(dppe)$, **6**.

Figure 5. Variable temperature ^1H spectra of a CD_2Cl_2 solution of $Ir(CO)_2(C(O)C_6H_2(CH_3)_3)(dppe)$, **6**. Region A = aromatic region, region B = dppe methylene region, ♦ = *p*-mesityl Me.

From the methylene region of the ^1H NMR spectrum, the rate constant at coalescence, k_{298}, for the interconversion is calculated to be 195.5 s^{-1} with a corresponding free energy of activation, $\Delta G^{\ddagger}$, of 14.3(2) kcal/mol.

Intramolecular Oxidative Addition of Benzylic C−H Bonds in 6. Formation of *trans*- and *cis*-IrH(CO)($CH_2C_6H_2(CH_3)_2C(O)$)(dppe) (7 and 8). A CD_2Cl_2 solution of **6** heated at 67 °C under 500 Torr of CO for 1.5 h yields an equilibrium between two new hydride-containing products, **7** and **8**, in a 1:1 ratio and complex **6** as determined by NMR spectroscopy (eq 6). Diastereotopic benzylic protons and hydride resonances consistent with *o*-methyl activation are displayed in the ^1H NMR spectrum while terminal and acyl carbonyl groups are identified in the $^{13}C\{^1H\}$ NMR spectrum (see Tables 1 and 2). A DEPT 135° NMR spectrum confirms the presence of benzylic carbons for complexes **7** and **8** as upfield signals at 2.81 and 11.2 ppm, respectively. On the basis of the spectroscopic data, **7** is assigned as *trans*-IrH(CO)($CH_2C_6H_2(CH_3)_2C(O)$)(dppe) with hydride trans to terminal carbonyl and **8** as *cis*-IrH(CO)-($CH_2C_6H_2(CH_3)_2C(O)$)(dppe) with hydride trans to phosphorus.

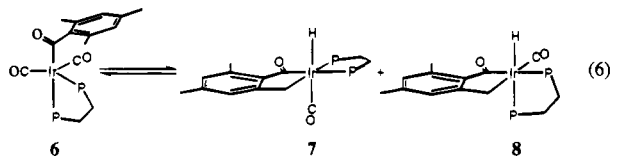

6 7 8 (6)

Complexes **7** and **8** are similar to those reported by Dahlenberg for $P(OMe)_3$-promoted cyclometalations of $IrR(CO)(PPh_3)_2$ (R = 2,6-$Et_2C_6H_3$, 2-Me,6-EtC_6H_3, 2,4,6-$Me_3C_6H_2$).[53,73-77] The formation of **7** and **8** can be envisioned to occur via CO loss from **6** to form the acyl intermediate **D**, followed by oxidative addition of a C−H *o*-methyl bond over either the P−Ir−CO axis, producing **7** or the P−Ir−acyl axis to yield **8**, as in Figure 4. The rate of product formation rules against an alternative mechanism which proceeds via the four-membered metallocycle hydride intermediate **A**, Figure 3, described for the formation of **2**.

The X-ray structure determination of **8** was carried out on a crystal grown from the slow evaporation of an acetone/diethyl ether solution of the equilibrium mixture. An ORTEP plot of **8** is shown in Figure 6. A listing of cystallographic data, intramolecular bond angles, and intramolecular bond distances for **8** are presented in Tables 3, 8 and 9, respectively. While the hydride atom was not located in the structure determination, its existence was established by the spectroscopic data and its position in the coordination sphere is evident. The geometry about iridium is that of a distorted octahedron with one of the dppe phosphine donors trans to the hydride ligand. The other dppe phosphorus, the carbonyl ligand, and the five-membered metallocycle ring occupy the remaining coordination sites. The Ir−P1 and Ir−P2 bond lengths of 2.344(2) and 2.364(2) Å, respectively, are similar and indicate that the hydride and acyl ligands have a similar structural trans influence on the phosphine donors. The iridium−benzyl bond of 2.141(6) Å is 0.07 Å shorter than the iridium−benzyl bond found in the Ir(I) complex **2** but is consistent with those found in the trimethyl phosphite derivatives.[77]

Reaction of Ir(Mes)(CO)(dppe) with SiH_2Ph_2. Formation of IrH($SiHPh_2$)(mes)(CO)(dppe) (9). A reaction at 0 °C between a toluene solution of Ir(Mes)(CO)(dppe) (**1**) and 1.1 equiv of SiH_2Ph_2 yields a new colorless complex (**9**) after 30 min of stirring under N_2 (eq 7). Complex **9** is isolated as an off-white solid in 65% yield upon solvent removal and addition of ethanol. The complex is characterized by infrared and NMR spectroscopies and microanalysis. The ^1H NMR spectrum confirms the presence of the hydride as a triplet at −8.42 ppm,

(73) Dahlenburg, L.; Mirzaei, F. *J. Organomet. Chem.* **1983**, *152*, 123−132.
(74) Dahlenburg, L. *J. Organomet. Chem.* **1983**, *251*, 215−222.
(75) Dahlenburg, L.; Mirzaei, F. *J. Organomet. Chem.* **1983**, *251*, 103−111.
(76) Arpac, E.; Dahlenburg, L. *Chem. Ber.* **1985**, *118*, 3188−3195.
(77) von Deuten, K.; Dahlenburg, L. *Transition Met. Chem.* **1980**, *5*, 222−225.

while the mesityl methyl groups display three separate signals indicative of hindered rotation of the mesityl ligand about the iridium–mesityl bond. Terminal CO coordination is established from ν_{CO} at 1968 cm^{-1}. On the basis of the spectroscopy and microanalyses, **9** is assigned as $IrH(SiHPh)_2(mes)(CO)(dppe)$. Equation 7 is an example of stereospecific oxidative addition of a Si–H bond of diphenylsilane over the CO–Ir–P axis of **1**.[46] The fact that this is the only isomer observed is consistent with the results reported previously for silane additions to [IrH(CO)(dppe)].[47]

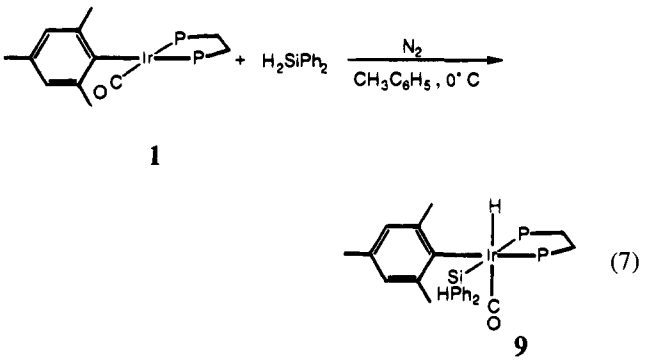

(7)

While in solution, **9** undergoes both irreversible mesitylene and reversible diphenylsilane reductive eliminations, leading to the formation of **1**, the bis(silyl) complex $IrH(SiHPh_2)_2(CO)(dppe)$, and mesitylene after several days (eq 8). The system thus exhibits competitive reductive elimination of aryl C–H and Si–H bonds, a detailed kinetic study of which will be described in a forthcoming publication.[48,69] The proposed intermediate formed from the reductive elimination of mesitylene, $[Ir(SiHPh_2)(CO)(dppe)]$, is not observed during the reaction but rather reacts rapidly with excess SiH_2Ph_2 to form the bis(silyl) product.

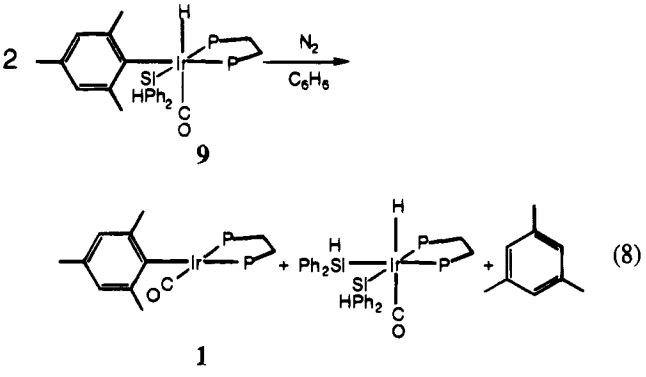

(8)

Reaction of Ir(mes)(CO)(dppe) with Dihydrogen. Formation of $IrH_2(mes)(CO)(dppe)$ (10). The reaction of **1** with H_2 at room temperature is rapid and irreversible. When a C_6D_6 solution of **1** is placed under 700 Torr of dihydrogen at ambient temperature, the immediate formation of the known complex $IrH_3(CO)(dppe)$ and free mesitylene is observed by ^1H NMR spectroscopy. The formation of both products can be explained by facile oxidative addition of dihydrogen to **1**, yielding $IrH_2(mes)(CO)(dppe)$ (**10**) followed by rapid reductive elimination of mesitylene. The proposed reductive elimination product, [IrH(CO)(dppe)], is not observed but is quickly trapped by a second equivalent of dihydrogen to form $IrH_3(CO)(dppe)$.

The existence of **10** was verified by placing a CD_2Cl_2 solution of **1** under 550 Torr of H_2 and allowing it to stand at −78 °C for 3 days (eq 9). Examination of the reaction solution by ^1H NMR spectroscopy at −20 °C exhibits two hydride resonances, both doublet of doublets, at −9.93 ($^2J_{H-P}$ = 132, 13 Hz) and

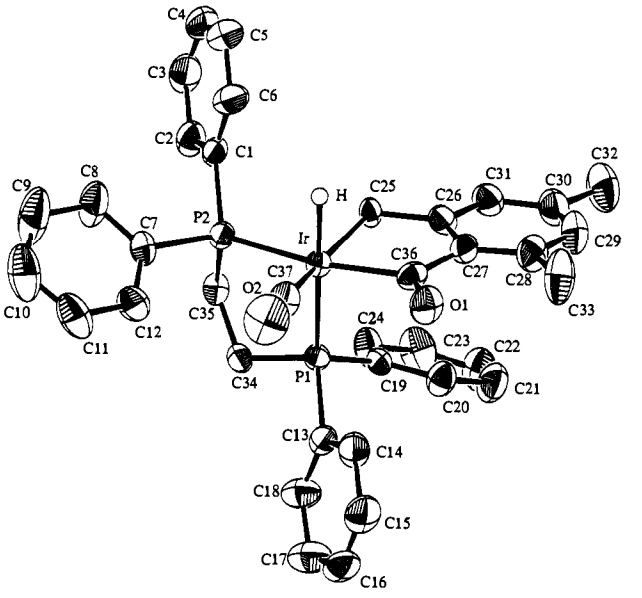

Figure 6. ORTEP plot of *cis*-$IrH(CO)(CH_2C_6H_2(CH_3)_2C(O))(dppe)$, **8**. Thermal ellipsoids shown at 50% probability. The hydride atom (H) is shown at a presumed position but was not located during structure solution.

Table 8. Selected Intramolecular Bond Angles (deg) for *cis*-$IrH(CO)(CH_2C_6H_2(CH_3)_2C(O))(dppe)$ (**8**)

atoms	angle	atoms	angle
P1–Ir–P2	85.01(6)	C25–C26–C31	121.6(6)
P1–Ir–C25	88.9(2)	C27–C26–C31	119.9(6)
P1–Ir–C36	97.0(2)	C26–C27–C28	119.0(6)
P1–Ir–C37	99.6(2)	C26–C27–C36	114.9(5)
P2–Ir–C25	87.7(1)	C28–C27–C36	125.9(6)
P2–Ir–C36	169.2(2)	C27–C28–C29	118.3(6)
P2–Ir–C37	99.9(2)	C27–C28–C33	121.8(7)
C25–Ir–C36	81.8(2)	C29–C28–C33	119.7(6)
C25–Ir–C37	169.0(3)	C28–C29–C30	123.3(6)
C36–Ir–C37	90.2(3)	C29–C30–C31	118.6(7)
Ir–P1–C13	121.2(2)	C29–C30–C32	119.9(7)
Ir–P1–C19	116.3(2)	C31–C30–C32	121.5(7)
Ir–P1–C34	107.7(2)	C26–C31–C30	120.8(6)
Ir–P2–C1	117.7(2)	Ir–C36–O1	125.3(5)
Ir–P2–C7	119.7(2)	Ir–C36–C27	114.4(4)
Ir–P2–C35	106.4(2)	O1–C36–C27	120.2(6)
Ir–C25–C26	109.7(4)	Ir–C37–O2	175.1(7)
C25–C26–C27	118.5(5)		

−10.06 (28, 19 Hz) ppm, indicating one hydride is trans and cis to dppe phosphorus nuclei while the other is cis to both dppe phosphorus atoms. In contrast to **9**, the *o*- and *p*-mesityl methyl groups appear as singlets in a 6:3 ratio, indicating free rotation about the iridium–mesityl bond. At temperatures above 0 °C and under H_2, **10** readily eliminates mesitylene with a measured $t_{1/2}$ = 20 min at 0 °C.

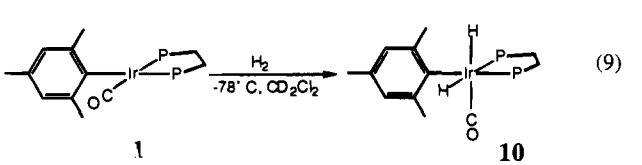

(9)

Dihydrogen addition occurs stereoselectively over the CO–Ir–P axis of **1** and is consistent with that observed previously for H_2 oxidative addition to Ir(X)(CO)(dppe) complexes where X = Cl, Br, I, H, CN.[44,45,78] Complex **10** does not display the PHIP effect, which suggests that reversible dihydrogen reductive

(78) Sargent, A. L.; Hall, M. B.; Guest, M. F. *J. Am. Chem. Soc.* **1992**, *114*, 517–522.

Table 9. Selected Intramolecular Bond Distances (Å) for *cis*-IrH(CO)($CH_2C_6H_2(CH_3)_2C(O)$)(dppe) (**8**)

atoms	distance	atoms	distance
Ir–P1	2.344(2)	C25–C26	1.502(8)
Ir–P2	2.364(2)	C26–C27	1.408(8)
Ir–C25	2.141(6)	C26–C31	1.410(9)
Ir–C36	2.073(6)	C27–C28	1.416(8)
Ir–C37	1.883(7)	C27–C36	1.488(9)
O1–C36	1.219(7)	C28–C29	1.38(1)
O2–C37	1.144(7)	C28–C33	1.52(1)
C1–C2	1.386(9)	C34–C35	1.525(8)

elimination/oxidative addition is not competitive with mesitylene reductive elimination.[79–82]

Reaction of Ir(mes)(CO)(dppe) with Molecular Iodine. Formation of Ir(C(O)$C_6H_2(CH_3)_3$)I_2(dppe) (11). The addition of 1.1 equiv of a benzene solution of molecular iodine to a benzene solution of **1** produced Ir(C(O)$C_6H_2(CH_3)_3$)I_2(dppe) (**11**) after precipitation from pentane in 84% yield (eq 10). Complex **11** is characterized by infrared and NMR spectroscopies, mass spectrometry, and microanalyses. Aryl migration is confirmed from the infrared spectrum, which displays an absorption band at 1664 cm^{-1} and an absence of bands between 2200 and 1900 cm^{-1}. The $^{31}P\{^1H\}$ NMR spectrum displays a singlet at 16.85 ppm, indicating equivalent phosphorus atoms while the FAB mass spectrum displays a parent ion peak (M^+) at 991. On the basis of the spectroscopic evidence, the solution structure of **11** is consistent with a square pyramid where the 1,3,5-trimethylbenzoyl ligand occupys the axial position and dppe and the two iodide ligands occupy the basal sites. The square pyramidal arrangement for **11** is consistent with that found in related five-coordinate Rh(III) and Ir(III) acyl complexes, including Rh(C(O)Et)I(PPh_3)(mnt)$^-$ (mnt = maleonitriledithiolate),[83] Rh(C(O)Et)(PEt_3)$_2$(mnt),[84] and Ir(C(O)Et)(PPh_3)$_2$(mnt).[85]

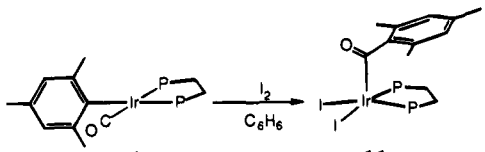

1 **11** (10)

The formation of **11** can be viewed to occur via polar oxidative addition of I_2 to **1** to generate [IrI(mes)(CO)(dppe)]$^+I^-$, which undergoes aryl migration to CO followed by coordination of I^- to the Ir(III) center. While the order of the last two steps is not established, it does seem evident that steric repulsion plays a role in the relative stability of the five-coordinate acyl **11** and the isomeric six-coordinate mesityl carbonyl species generated by I_2 oxidative addition alone. Equation 10 may thus be viewed as an oxidative addition of iodine with concomitant iodide-promoted carbonylation.[86,87]

Reaction of Ir(mes)(CO)(dppe) with Hydrogen Chloride. Formation of $IrHCl_2$(CO)(dppe) (12). The addition of excess hydrogen chloride gas to a CD_2Cl_2 solution of **1** at −78 °C leads to the immediate formation of a colorless solution of complex **12** and mesitylene (eq 11). The ^1H NMR spectrum of **12** displays a doublet of doublets ($^2J_{H-P}$ = 14.0, 11.7 Hz) at −16.73, confirming the presence of a hydride ligand cis to two phosphorus donors while a singlet at 2.20 ppm establishes liberated mesitylene. Two inequivalent cis phosphorus atoms are present in the $^{31}P\{^1H\}$ NMR spectrum, and ν_{CO} at 2075 cm^{-1} is consistent with a terminal carbonyl ligand bonded to iridium(III). On the basis of the spectroscopic data and microanalyses, complex **12** is assigned as the previously reported complex $IrHCl_2$(CO)(dppe).[46]

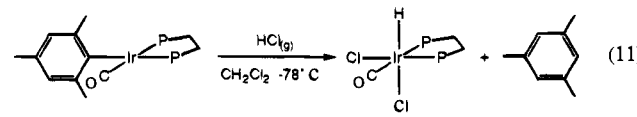

1 **12** (11)

Although no intermediates are observed when eq 11 is monitored by low-temperature NMR spectroscopy, the formation of **12** and mesitylene undoubtedly occurs via HCl oxidative addition to **1**, yielding the hydrido mesityl intermediate IrHCl(mesityl)(CO)(dppe) followed by facile reductive elimination of mesitylene and subsequent oxidative addition of a second hydrogen chloride to IrCl(CO)(dppe).[46]

Summary

Establishing the structure and chemical reactivity of **1** and model complexes like **1** provides a means for modeling catalytic cycles in a stepwise fashion. The reactions presented here detail both transformations and species thought to be significant in homogeneously catalyzed hydrogenations, hydrosilations, and hydroformylations. An important feature of the chemistry described here pertains to the *o*-methyl groups of the mesityl ligand. These groups serve to block access to Ir coordination by ethylene but not to H_2 and SiH_2Ph_2 for concerted oxidative addition reactions or to CO for coordination. The proximity of the mesityl *o*-methyl groups also renders them susceptible to C–H activation, leading to the unusual mesityl to dimethylbenzyl transformation and the formation of 4- and 5-membered metallocycles.

The oxidative additions of diphenylsilane, molecular hydrogen, and hydrogen chloride to **1** are consistent with that seen for other Ir(I) dppe complexes, and for the first two substrates, it appears to proceed stereoselectively. The resultant six-coordinate Ir(III) hydride mesityl products undergo facile reductive elimination of mesitylene. In all of the six-coordinate Ir(III) species, the coordination sphere is spatially arranged to make possible competitive reductive elimination reactions. These reactions may be able to probe the relative tendency of different reductive eliminations such as C–H vs Si–H elimination from **9** and aryl C–H vs benzyl C–H elimination from **A** in the reaction leading to the formation of **2**. The Ir–mesityl bond also undergoes migratory insertion of CO readily upon the addition of CO to the system, and surprisingly, after oxidation by molecular iodine.

Experimental Section

Reactions and sample preparations were completed in a nitrogen-filled glovebox or under the appropriate gas using a high-vacuum line or Schlenk line. All solvents were reagent grade or better and were dried and degassed prior to use by accepted methods.[88] Ethylene

(79) Eisenschmid, T. C.; Kirss, R. U.; Deutsch, P. P.; Hommeltoft, S. I.; Eisenberg, R.; Bargon, J.; Lawler, R. G.; Balch, A. L. *J. Am. Chem. Soc.* **1987**, *109*, 8089–8091.
(80) Eisenschmid, T. C.; McDonald, J.; Eisenberg, R. *J. Am. Chem. Soc.* **1989**, *111*, 7267–7269.
(81) Eisenberg, R. *Acc. Chem. Res.* **1991**, *24*, 110–116.
(82) Eisenberg, R.; Eisenschmid, T. C.; Chinn, M. S.; Kirss, R. U. *Adv. Chem. Ser.* **1992**, *230*, 47–74.
(83) Cheng, C.-H.; Spivack, B. D.; Eisenberg, R. *J. Am. Chem. Soc.* **1977**, *99*, 3003.
(84) Cheng, C.-H.; Eisenberg, R. *Inorg. Chem.* **1979**, *18*, 1418–1424.
(85) Anderson, D. J.; Eisenberg, R. To be submitted.
(86) Morrison, E. D.; Geoffroy, G. L. *J. Am. Chem. Soc.* **1985**, *107*, 3541–3545.
(87) Earle, A.; Jablonski, C. R. *J. Chem. Soc., Dalton Trans.* **1986**, 2137–2143.
(88) Perrin, D. D.; Armarego, W. L. F. *Purification of Laboratory Chemicals*, 3rd ed.; Pergamon Press: Oxford, England, 1988; p 391.

(99.8%, Air Products), carbon monoxide (99.3%, Air Products), ^{13}C-labeled carbon monoxide (99%, Cambridge), hydrogen (99.99%, Air Products), and hydrogen chloride (99%, Air Products) were used as received. New bottles of mesitylmagnesium bromide (1.0 M in tetrahydrofuran, Aldrich), *o*-tolylmagnesium bromide (2.0 M in diethyl ether, Aldrich), benzylmagnesium bromide (2.0 M in tetrahydrofuran, Aldrich) and 33−36% aqueous hydrochloric acid (Fisher) were used as received. Diphenylsilane (Hüls of America) and phenylsilane (Hüls of America) were dried over calcium hydride (Aldrich), vacuum transferred, and stored under nitrogen in an amber bottle. IrBr(CO)(dppe) was prepared according to literature procedures.[44]

Most NMR samples were prepared using resealable NMR tubes fitted with J Young Teflon valves (Brunfeldt) and high vacuum line adapters. Otherwise, samples were placed in NMR tubes with high-vacuum line adapters and flame sealed after solvent transfer. Stoichiometric amounts of gases were delivered to NMR samples by measuring the internal volume of the NMR tube and calculating the corresponding pressure using the ideal gas law. ^1H, ^{13}C, and ^{31}P NMR spectra were recorded at 400.13, 100.62, and 161.98 MHz, respectively, on a Bruker AMX 400 NMR spectrometer. Temperature control was achieved using a B-VT 1000 variable temperature unit and a Cu−constantan temperature sensor that was calibrated for high and low temperatures using ethylene glycol and methanol standards, respectively. ^1H NMR chemical shifts are reported in ppm downfield of tetramethylsilane but measured from residual ^1H signal in the deuterated solvents. ^{13}C NMR spectra are reported in ppm downfield of tetramethylsilane and referenced to a known carbon signal in the solvent. ^{31}P NMR spectra are reported in ppm downfield of an external 85% solution of phosphoric acid. Benzene-d_6 (MSD) and toluene-d_8 (Cambridge) were dried and distilled from purple solutions of sodium benzophenone ketyl. Methylene chloride-d_2 (Cambridge) was dried and distilled from a calcium hydride suspension. Solution and KBr (Aldrich) mull infrared spectra were recorded on a Matteson 6020 Galaxy FT-infrared spectrometer. Fast atom bombardment (FAB) mass spectra were collected on a VG Analytical TS-250 mass spectrometer. Elemental analyses were performed by Desert Analytics Laboratory, Tucson, AZ.

Ir(mes)(CO)(dppe) (1). To a cooled (−78 °C) tetrahydrofuran (60 mL) solution of IrBr(CO)(dppe) (250 mg, 0.358 mmol) containing a magnetic stir bar was added 2 equiv of a 1.0 M (0.72 mL, 0.716 mmol) tetrahydrofuran solution of mesitylmagnesium bromide. The solution was allowed to warm to room temperature and stirred for 1 h, after which 1 equiv of *p*-dioxane was added to neutralize excess Grignard. The solvent was removed *in vacuo*, and the residue was extracted with diethyl ether. Precipitation of the product was achieved by the slow addition of ethanol to a concentrated ether solution of **1**. Recrystallization from diethyl ether/ethanol yielded **1** as air-stable, orange microcrystals in 69% yield.

Anal. Calcd for $C_{36}H_{35}IrOP_2$: C, 58.60; H, 4.78. Found: C, 58.32; H, 4.81.

Ir(η^2-C_2H_4)($CH_2C_6H_3(CH_3)_2$)(CO)(dppe) (2). To a Schlenk tube were added **1** (100 mg, 0.136 mmol), 5 mL of benzene, a magnetic stir bar, and 700 Torr of ethylene. The solution was stirred at 90 °C for 7 days and then transferred to a 10-mL Erlenmeyer flask, where the volume was concentrated to 1 mL by slow evaporation. Following the addition of 5 mL of a 1:1 solution of diethyl ether/ethanol and cooling to −35 °C, yellow crystals of **2** were obtained in 70% yield.

Anal. Calcd for $C_{38}H_{39}IrOP_2$: C, 59.59; H, 5.13. Found: C, 58.11; H, 4.88. Unsatisfactory analysis was due in part to the facile loss of coordinated ethylene upon drying.

Ir(C_6F_5)(CO)(dppe) (3). A tetrahydrofuran solution of (pentafluorophenyl)magnesium bromide (0.42 M) was prepared by the slow addition of bromopentafluorobenzene (10 mL, 80.2 mmol) to 200 mL of tetrahydrofuran containing 1 equiv of magnesium filings (1.95 g; 80.2 mmol). To a cooled (−78 °C) tetrahydrofuran (50 mL) solution of IrBr(CO)(dppe) (203 mg, 0.290 mmol) containing a magnetic stir bar was added 1.5 equiv of the 0.42 M (1.0 mL, 0.316 mmol) tetrahydrofuran solution of (pentafluorophenyl)magnesium bromide. The solution was allowed to warm to room temperature and stirred for 4 h, after which 1 equiv of *p*-dioxane was added to neutralize excess Grignard. The solvent was removed *in vacuo*, and the residue was extracted with benzene. Precipitation of the product was achieved by the slow addition of diethyl ether to a concentrated benzene solution of **3**. Recrystallization from benzene/diethyl ether yielded **3** as an orange-yellow powder in 75% yield.

Ir(*o*-tolyl)(CO)(dppe) (4). To a cooled (−78 °C) tetrahydrofuran (50 mL) solution of IrBr(CO)(dppe) (144 mg, 0.206 mmol) containing a magnetic stir bar was added 1.1 equiv of a 2.0 M (0.11 mL, 0.22 mmol) diethyl ether solution of *o*-tolylmagnesium bromide. The solution was allowed to warm to room temperature and stirred for 1 h, after which 1 equiv of *p*-dioxane was added to neutralize excess Grignard. The solvent was removed *in vacuo*, and the residue was extracted with benzene. Precipitation of the product was achieved by the slow addition of ethanol to a concentrated benzene solution of **4**. Recrystallization from diethyl ether/ethanol yielded **4** as an orange powder in 71% yield.

Ir(benzyl)(CO)(dppe) (5). To a cooled (−78 °C) tetrahydrofuran (50 mL) solution of IrBr(CO)(dppe) (154 mg, 0.221 mmol) containing a magnetic stir bar was added 1.2 equiv of a 2.0 M (0.13 mL, 0.265 mmol) tetrahydrofuran solution of benzyl magnesium bromide. The solution was allowed to warm to room temperature and stirred for 3 h, after which 1 equiv of *p*-dioxane was added to neutralize excess Grignard. The solvent was removed *in vacuo*, and the residue was extracted with toluene. Precipitation of the product was achieved by the slow addition of ethanol to a concentrated toluene solution of **5**. Recrystallization from diethyl ether/ethanol yielded **5** as a brick-red powder in 65% yield.

NMR-Scale Ethylene Additions to 3, 4, and 5. The general procedure utilized a resealable NMR tube containing 5 mg of the appropriate four-coordinate Ir(I) complex dissolved in 0.5 mL of degassed C_6D_6. The tube was immersed in a dry ice/acetone bath, placed under 700 Torr of ethylene, and thawed, and the reaction was monitored by NMR spectroscopy, Table 1 and 2.

Ir($CO)_2$($C(O)C_6H_2(CH_3)_3$)(dppe) (6). A 50 mL round bottom flask containing a magnetic stir bar and **1** (100 mg, 0.136 mmol) was pump flushed with CO three times prior to the addition of 10 mL of degassed (CO) dichloromethane. The resulting colorless solution was stirred for 5 min and cooled to 0 °C. Complex **8** was isolated in 80% yield as an off-white solid after precipitation by the addition of 25 mL of cold, degassed (0 °C, CO) hexanes.

Anal. Calcd for $C_{38}H_{35}IrO_3P_2$: C, 57.49; H, 4.44. Found: C, 57.56; H, 4.45.

Formation of *trans*- and *cis*-IrH(CO)($CH_2C_6H_2(CH_3)_2C(O)$)(dppe) (7 and 8). A resealable NMR tube charged with 5 mg of **8** and 0.5 mL of C_6D_6 was put through three freeze/pump/thaw cycles and then placed under 550 Torr of CO. After 1.5 h of heating at 67 °C, two new hydride-containing species were observed in apparent equilibrium with **6**.

Ir$H(SiHPh_2)_2$(CO)(mes)(dppe) (9). Complex **1** (50 mg, 0.0683 mmol) was placed in 1 mL of toluene along with a magnetic stir bar and cooled to 0 °C. To the orange solution was added 1.1 equiv (14.0 μL, 0.0751 mmol) of diphenylsilane. After 2 min of stirring, the solution became colorless. The product precipitated after the addition of 6 mL of ethanol and reduction of the volume to 3 mL under a stream of nitrogen. After an additional 3 mL of ethanol was added, the product was isolated as an air-stable, cream-colored powder in 65% yield.

Unassigned aromatic resonances, ^1H NMR (C_6D_6): δ 7.86 (m, 2H, Ph), 7.58 (d, 2H, Ph), 7.53 (m, 2H, Ph), 7.45 (m, 2H, Ph), 7.23 (m, 2H, Ph), 7.13−7.00 (m, 12 H, Ph), 6.91 (m, 4H, Ph), 6.81 (m, 3H, Ph), 6.75 (m, 3H, Ph).

Anal. Calcd for $C_{48}H_{47}IrOP_2Si$: C, 62.45; H, 5.13. Found: C, 62.64; H, 5.12.

IrH_2(CO)(mes)(dppe) (10). Due to the facile reductive elimination of mesitylene from **10**, NMR spectroscopy was used for characterization. In an NMR tube fitted with a high-vacuum line adapter was placed 7 mg of **1**. Approximately 0.5 mL of dichloromethane-d_2 was vacuum transferred to the tube followed by 550 Torr of dihydrogen. The tube was flame sealed, transferred to a dry ice−acetone bath, and allowed to react for 3 days, after which time NMR spectroscopy indicated that the reaction was 100% complete.

IrI_2($C(O)C_6H_2(CH_3)_3$)(dppe) (11). To a 50 mL round bottom flask charged with **1** (100 mg, 0.136 mmol), a magnetic stirbar, and 10 mL of benzene was added 1.1 equiv of a 0.12 M (1.25 mL, 0.150 mmol) benzene solution of iodine. The orange solution of **1** quickly lightened to pale orange, and a pale orange precipitate formed after a few minutes

of stirring. The addition of 20 mL of cold pentane completed the precipitation. Complex **11** was isolated as an air-stable pale powder complex after recrystallization from dichloromethane and pentane in 84% yield. Alternatively, **11** could be purified via preparative thin layer chromatography using a 30:1 solution of dichloromethane: benzene. FAB MS, *m/z* 991 (M^+).

Anal. Calcd for $C_{36}H_{35}I_2IrOP_2$: C, 43.62; H, 3.66; I, 26.34. Found: C, 43.94; H, 3.73; I, 25.74.

Reaction of 1 with HCl. Formation of $IrHCl_2(CO)(dppe)$ (12). To an NMR tube fitted with a high-vacuum line adapter was added 5 mg (6.8×10^{-3} mmol) of **1**. The tube was placed on a high-vacuum line where ca. 0.5 mL of toluene-d_8 was vacuum transferred and kept frozen in a liquid nitrogen bath. The frozen solution was exposed to 63 Torr of HCl gas (6.8×10^{-3} mmol), flame sealed, and thawed in a dry ice−acetone bath. Insertion of the tube into a precooled (−75 °C) NMR probe showed **12** and mesitylene as the only products.

On a larger scale, a 50 mL round bottom flask was charged with a magnetic stir bar, **1** (50 mg, 0.068 mmol), and 1 mL of benzene. The benzene solution was treated with 3 drops of 33−36% aqueous HCl and stirred for 15 min, after which an off-white solid was observed to precipitate. Following the addition of 20 mL of pentane, the air-stable product was isolated in 91% yield.

Anal. Calcd for $C_{27}H_{25}Cl_2IrOP_2$: C, 46.96; H, 3.65. Found: C, 46.75; H, 3.67.

X-ray Crystallography, General. Crystal data and data collection and refinement parameters for Ir(mes)(CO)(dppe)(**1**), Ir(η^2-C_2H_4)($CH_2C_6H_3(CH_3)_2$)(CO)(dppe)·$^1/_2C_2H_5OH$ (**2**), and *cis*-IrH(CO)($CH_2C_6H_2(CH_3)_2$C(O))(dppe) (**8**) are summarized in Table 3. All structures were determined by gluing a crystal of the desired compound to a glass fiber using five-minute epoxy, and mounting the goniometer head on an Enraf-Nonius CAD4 diffractometer with graphite-monochromated Mo Kα radiation operating in the $\omega/2\theta$ scan mode. For each crystal, cell constants and an orientation matrix for data collection were obtained from a least-squares refinement using the setting angles of 25 carefully centered reflections. For each crystal determination, an empirical absorption correction, using the program DIFABS, was applied.[89] Neutral atom scattering factors were taken from Cromer and Waber.[90] Anomalous dispersion effects were included in F_{calc}; the values for $\Delta f'$ and $\Delta f''$ were those of Cromer.[91] All calculations were performed using TEXSAN software.[92]

X-ray Structure Determination of Ir(mes)(CO)(dppe) (1). Orange crystals of **1** were grown by the slow evaporation of a saturated toluene solution at −35 °C. A broken needle (0.34 × 0.26 × 0.23 mm) was used for data collection at 0 °C. Of the 4438 reflections collected, 4128 were unique ($R_{int} = 0.056$). Representative reflections showed no decay during acquisition, indicating crystal stability. The structure was solved by a combination of Patterson and direct methods. The nonhydrogen atoms were refined anisotropically while all hydrogen atoms were placed in calculated positions with B_{iso} equivalent to 1.2 × B_{iso} of the bonded nonhydrogen atom. Hydrogen atom positions were updated after all but the final cycle of least-squares refinements. The final cycle of full-matrix least-squares refinement was based on 2333 observed reflections ($I > 3.00\sigma(I)$) and 361 variable parameters and converged with unweighted and weighted agreement factors of $R = \sum||F_o| - |F_c||/\sum|F_o| = 0.032$ and $R_w = [(\sum w(|F_o| - |F_c|)^2/wF_o^2)]^{1/2} = 0.033$ with a maximum shift/esd of 0.58. The maximum and minimum peaks on the final difference Fourier map corresponded to 0.467 and −0.474 e⁻/Å³, respectively.

X-ray Structure Determination of Ir(η^2-C_2H_4)($CH_2C_6H_3(CH_3)_2$)(CO)(dppe)·$^1/_2$ C_2H_5OH. Yellow crystals of **2** were grown by the slow evaporation of a toluene/diethyl ether/ethanol solution at −35 °C. A needle that was halved (0.49 × 0.19 × 0.15 mm) was used for data collection at 0 °C. All of the 4890 reflections collected were unique. Representative reflections showed no decay during acquisition, indicating crystal stability. The iridium atom was located by the Patterson method and successive difference Fourier maps and least-squares refinements were used to locate the remaining non-hydrogen atoms. A disordered molecule of ethanol was modeled by fixing the isotropic thermal parameters for these atoms and refining their populations by least-squares refinement to convergence. All non-hydrogen atoms were refined anisotropically except for the atoms corresponding to the disordered ethanol molecule which were refined isotropically. All hydrogen atoms were placed in calculated positions with B_{iso} equivalent to 1.2 × B_{iso} of the bonded non-hydrogen atom. Hydrogen atom positions were updated after all but the final cycle of least-square refinements. The final cycle of full-matrix least-squares refinement was based on 2667 observed reflections ($I > 3.00\sigma(I)$) and 391 variable parameters and converged with unweighted and weighted agreement factors of $R = \sum||F_o| - |F_c||/\sum|F_o| = 0.034$ and $R_w = [(\sum w(|F_o| - |F_c|)^2/wF_o^2)]^{1/2} = 0.038$ with a maximum shift/esd of 0.094. The maximum and minimum peaks on the final difference Fourier map corresponded to 0.651 and −0.408 e⁻/Å³, respectively.

X-ray Structure Determination of *cis*-IrH(CO)($CH_2C_6H_2(CH_3)_2$C(O))(dppe) 8. Pale yellow crystals of **8** were grown by the slow evaporation of a saturated acetone/diethyl ether solution at room temperature in air. A parallelepiped (0.60 × 0.34 × 0.53 mm) was used for data collection at 0 °C. Of the 6459 reflections collected, 5937 were unique ($R_{int} = 0.036$). Representative reflections showed no decay during aquisition, indicating crystal stability. The iridium atom was located by the Patterson method, and direct methods was used to locate the remaining non-hydrogen atoms. The non-hydrogen atoms were refined anisotropically while all hydrogen atoms were placed in calculated positions with B_{iso} equivalent to 1.2 × B_{iso} of the bonded non-hydrogen atom. Hydrogen atom positions were updated after all but the last least-squares refinements. The final cycle of full-matrix least-squares refinement was based on 4050 observed reflections ($I > 3.00\sigma(I)$) and 379 variable parameters and converged with unweighted and weighted agreement factors of $R = \sum||F_o| - |F_c||/\sum|F_o| = 0.029$ and $R_w = [(\sum w(|F_o| - |F_c|)^2/wF_o^2)]^{1/2} = 0.032$ with a maximum shift/esd of 0.04. The maximum and minimum peaks on the final difference Fourier map corresponded to 0.581 and −0.768 e⁻/Å³, respectively.

Acknowledgment. We wish to thank the National Science Foundation (Grants CHE 89-09060 and CHE 94-04991) for support of this work, the Johnson Matthey Co., Inc. for a generous loan of iridium trichloride, and Mr. Terry O'Connell for providing assistance in acquiring the FAB mass spectrum. B.P.C. gratefully acknowledges Sherman Clarke, Bristol Myers-Squibb, and Arnold Weissberger Fellowships.

Supplementary Material Available: Tables of bond angles, bond lengths, positional and equivalent isotropic thermal parameters, and anisotropic thermal parameters for complexes **1**, **2**, and **8**, $^{13}C\{^1H\}$ NMR data for complexes **1**, **2**, **3**, **9**, and **12**, and an excerpt of the double quantum filtered COSY NMR spectrum of **2** (28 pages). This material is contained in many libraries on microfiche, immediately follows this article in the microfilm version of the journal, can be ordered from the ACS, and can be downloaded from the Internet; see any current masthead page for ordering information and Internet access instructions.

JA943341J

(89) Walker, N.; Stuart, D. *Acta Crystallogr.* **1983**, *A29*, 158−166.
(90) Cromer, D. T.; Waber, J. T. *International Tables for X-ray Crystallography*; The Kynoch Press: Birmingham, England, 1974; Vol. IV, Table 2.2 A.
(91) Cromer, D. T. *International Tables for X-ray Crystallgraphy*; The Kynoch Press: Birmingham, England, 1974; Vol. IV, Table 2.3.1.
(92) TEXSAN-TEXRAY Structure Analysis Package. Molecular Structure Corporation, 1985.